HBXIP knockdown inhibits FHL2 to promote cycle arrest and suppress cervical cancer cell proliferation, invasion and migration

XIA GAO[1] and LINA YANG[2]

[1]Department of Gynaecology, Heping Hospital Affiliated to Changzhi Medical College, Changzhi, Shanxi 046000; [2]Department of Gynecology, The 521 Hospital of Norinco Group, Xi'an, Shaanxi 710065, P.R. China

Received July 4, 2022; Accepted December 7, 2022

DOI: 10.3892/ol.2023.13772

Abstract. Hepatitis B X-interacting protein (HBXIP) and four and a half LIM domain 2 (FHL2) have been reported to serve as independent biomarkers for cervical cancer. The present study evaluated the effects of HBXIP on cervical cancer in terms of its cellular malignant characteristics. Reverse transcription-quantitative PCR and western blotting were used to assess the mRNA and protein expression levels of HBXIP and FHL2 in the human endocervical epithelial End1/E6E7 cell line and the cervical cancer HeLa, CaSki, C33A and SiHa cell lines. After knocking down HBXIP expression by transfection of small interfering RNAs targeting HBXIP, cell cycle progression was assessed using flow cytometry with PI staining. Cell Counting Kit-8, 5-ethynyl-2'-deoxyuridine staining, wound healing and Transwell assays were used to assess cell proliferation, migration and invasion, respectively. Furthermore, co-immunoprecipitation assay was used to evaluate the potential binding relationship between HBXIP and FHL2. Western blotting was used for the analysis of HBXIP and FHL2, cell cycle-associated proteins, including cyclin D1 and cyclin D2, metastasis-associated proteins, including MMP2 and MMP9, and Wnt/β-catenin signaling-associated proteins, including β-catenin and c-Myc. Both HBXIP and FHL2 were found to be highly expressed in cervical cancer cells compared with that in the human endocervical epithelial cell line. HBXIP knockdown suppressed the proliferation, invasion and migration of HeLa cells, but promoted cell cycle arrest at the G_0/G_1 phase. HBXIP was demonstrated to interact with FHL2, and HBXIP knockdown also inhibited FHL2 mRNA and protein expression. By contrast, FHL2 overexpression reversed the inhibitory effects of HBXIP knockdown on the malignant characteristics of cervical cancer cells. Furthermore, HBXIP knockdown blocked the Wnt/β-catenin signaling pathway in HeLa cells, which was also partially reversed by FHL2 overexpression; the decreased β-catenin and c-Myc expression caused by HBXIP knockdown was increased again after FHL2 was overexpressed. In conclusion, these results suggest that HBXIP knockdown suppressed the malignant characteristics of cervical cancer cells through the downregulation of FHL2 expression, indicating a promising insight into the therapeutic target of cervical cancer.

Introduction

Cervical cancer is a malignancy in women that can result from persistent infection with the high-risk human papillomavirus and has a high mortality rate, especially in low and middle-income countries (1). In 2020, the estimated cervical cancer mortality rate across all 78 LMICs was 13.2 (range, 12.9-14.1) per 100 000 women (2). First occurrence of sexual intercourse at younger ages, increase in the number of sexual partners, smoking, long-term use of oral contraceptives and viral infections can all increase the risk of cervical cancer (3). Screening, vaccination, preventive education and physical examination programs have all decreased the prevalence of cervical cancer. However, women with this disease do not have access to curative treatment, since there is no adequate and effective method to treat cervical cancer due to relapse, metastasis and drug resistance (1,4). Therefore, the mechanism underlying cervical carcinogenesis must be elucidated to aid in the development of effective treatment modalities.

Hepatitis B X-interacting protein (HBXIP) has been previously reported to serve as a carcinogenic factor in numerous cancer types, including hepatocellular carcinoma, breast cancer, gastric cancer and colorectal cancer (5-9). Its carcinogenic effects have been demonstrated to involve a variety of complex mechanisms, including the promotion of mitosis to sustain tumor cell proliferation, activation of transcription factors to regulate the cancer cell phenotype and the induction of signaling pathways to promote cancer development (10). Over the past two decades, high expression levels of HBXIP have been reported in hepatocellular carcinoma, breast cancer, gastric cancer and colorectal cancer, which are in turn associated with poorer prognosis (6-9). In particular, it has been also been previously reported that the HBXIP expression levels are elevated in cervical cancer tissues, which is associated with worse prognosis (11). However, the exact mechanism of action

Correspondence to: Dr Xia Gao, Department of Gynaecology, Heping Hospital Affiliated to Changzhi Medical College, 110 Yan'an South Road, Luzhou, Changzhi, Shanxi 046000, P.R. China
E-mail: gaoxiagx11@126.com

Key words: hepatitis B X-interacting protein, four and a half LIM domain 2, cervical cancer, proliferation

mediated by HBXIP remains unelucidated (11). Therefore, evaluation of the specific mechanism of action of HBXIP in cervical cancer may enrich the target pool for cervical cancer therapy and provide novel approaches for the cancer therapeutic interventions.

The novel LIM domain protein four and a half LIM domain 2 (FHL2) is encoded by the human FHL2 gene (12). The reported role of FHL2 in cancer biology remains controversial. FHL2 expression has been reported to be downregulated in prostate cancer, rhabdomyosarcoma and hepatocellular carcinoma (13-15), but it has also been reported to be upregulated in epithelial ovarian cancer, human hearts and human melanoma (16-18). Previous studies have reported that FHL2 expression was higher in squamous cervical tissues compared with that in non-cancerous cervical tissues, where its high expression was associated with poorer prognosis (19,20). In addition to its high affinity with cancer-associated proteins, FHL2 can also regulate signaling pathways associated with the malignant transformation of cells (21). Furthermore, FHL2 knockdown has been reported to suppress the activation of Wnt signaling, which has been frequently reported to be involved in the malignant transformation of cervical cancer (22). Based on the observations made by these aforementioned previous studies, the present study evaluated whether HBXIP can bind to the FHL2 protein and exert effects on the Wnt signaling pathway in cervical cancer.

To support this evaluation, the present study assessed the mRNA and protein expression levels of HBXIP and FHL2 in cervical cancer cells, evaluated how HBXIP influenced the malignant development of cervical cancer cells and assessed whether FHL2 overexpression affected these results. This investigation might offer potential novel targets for cervical cancer treatment.

Materials and methods

Bioinformatics tools. The BioGRID database (https://thebiogrid.org/) was used by searching the interactors of HBXIP to predict the relationship between FHL2 and HBXIP.

Cell culture. The human endocervical epithelial End1/E6E7 cell line, the human cervical cancer HeLa, C33A and SiHa cell lines, and the cervical squamous cell carcinoma Ca-Ski cell line were purchased from BioVector NTCC, Inc. End1/E6E7 cells were cultured in keratinocyte serum-free medium (Gibco; Thermo Fisher Scientific, Inc.) supplemented with 50 μg/ml bovine pituitary extract (Absin Bioscience, Inc.), 0.1 ng/ml recombinant epidermal growth factor (Absin Bioscience, Inc.), 0.4 mmol/l $CaCl_2$ and 1% antibiotics (penicillin, 100 U/ml; streptomycin, 100 mg/ml). HeLa and CaSki cervical cancer cell lines were cultured in RPMI-1640 (Procell Life Science & Technology Co., Ltd.) containing 10% fetal bovine serum (Invitrogen; Thermo Fisher Scientific, Inc.) and 1% penicillin-streptomycin. C33A and SiHa cells were cultured in DMEM (MilliporeSigma) containing 10% fetal bovine serum (Invitrogen; Thermo Fisher Scientific, Inc.) and 1% penicillin-streptomycin. All cells were cultured under the conditions of 37˚C with 5% CO_2.

Cell transfection. Small interfering RNAs (siRNA) targeting HBXIP (siRNA-HBXIP-1, 5'-GTGATGTTTTCCAGTAAAGAACG-3'; and siRNA-HBXIP-2, 5'-CAGATAATGGGAACATTATGATC-3') and the non-targeting control (siRNA-NC, 5'-AAGACAUUGUGUGUCCGCCTT-5') were supplied by Santa Cruz Biotechnology, Inc. The pcDNA3.1 vector containing the full-length cDNA sequence of FHL2 (Ov-FHL2) and the empty vector (Ov-NC) were supplied by Shanghai GenePharma Co., Ltd. siRNAs (5 nM) and overexpression plasmids (50 nM) were transfected into HeLa cells using a Lipofectamine® 2000 kit (Invitrogen; Thermo Fisher Scientific, Inc.) for 48 h at 37˚C according to the manufacturer's protocols. At 48 h post-transfection, the transfected cells were harvested for use for subsequent experiments.

Cell Counting Kit-8 (CCK-8) assay. HeLa cells were inoculated into 96-well plates ($2x10^3$ cells/well) and were cultured at 37˚C with 5% CO_2 for 24, 48 or 72 h. Following the addition of 10 μl CCK-8 solution (Shanghai Yeasen Biotechnology Co., Ltd.), cells were cultured at 37˚C for 3 h. A microplate reader (Bio-Rad Laboratories, Inc.) was then used to assess the absorbance in each well at 450 nm.

5-ethynyl-2'-deoxyuridine (EDU) staining. Cell proliferation was evaluated using a BeyoClick™ EdU Cell Proliferation Kit (cat. no. C0085S; Beyotime Institute of Biotechnology). HeLa cells were seeded into 96-well plates at $1x10^4$ cells/well. At 48 h post-transfection, 100 μl EdU solution was added into each well and the cells were cultured at 37˚C with 5% CO_2 for 2 h. HeLa cells were then fixed using 4% paraformaldehyde at room temperature for 10 min and permeabilized using 0.3% Triton X-100 for 15 min at room temperature. After washing with PBS, HeLa cells were incubated with a Click reaction solution for 30 min in the dark at room temperature. Finally, the nuclear DNA was stained with DAPI (5 μg/ml; Beyotime Institute of Biotechnology) for 10 min at room temperature. Cells were imaged using a fluorescence microscope (Olympus Corporation).

Wound healing assay. The migratory capacity of the cells was assessed using a wound healing assay. The HeLa cells were inoculated into six-well plates at $4x10^5$ cells/well and cultured at 37˚C. Upon reaching ~95% confluence, a sterile 200-μl pipette tip was used to scratch the cells to create a wound in the cell monolayer. After washing with PBS, cells were incubated with serum-free RPMI-1640 medium for 48 h at 37˚C. Images at 0 and 48 h were captured using a light microscope (Olympus Corporation). The relative cell migration rate of each group (scratch distance at 24 h-initial distance at 0 h) was normalized according to the average migrated distance of the control group and analyzed using ImageJ software 1.52r (National Institutes of Health).

Transwell assay. HeLa cells ($5x10^4$ cells/well) were resuspended in serum-free RPMI-1640 medium and were seeded into the upper chambers of Transwell plates (pore size, 8 mm; BD Biosciences), which were pre-coated with 60 μl Matrigel (2 mg/ml; BD Biosciences) for 1 h at room temperature. Complete RPMI-1640 medium (500 μl; Procell Life Science & Technology Co., Ltd.) containing 10% FBS (Invitrogen; Thermo Fisher Scientific, Inc.) was added into the lower chamber. After 48 h incubation at 37˚C with 5% CO_2, a cotton

swab was used to remove the cells from the upper chamber. Cells that penetrated the membranes were fixed using 4% paraformaldehyde for 10 min at room temperature and stained using 0.1% crystal violet for 15 min at room temperature. The number of invasive cells in five randomly selected fields of view were then assessed using a light microscope (Olympus Corporation) and quantified using ImageJ software 1.52r (National Institutes of Health).

Flow cytometry. HeLa cells were harvested by trypsinization using 0.05% trypsin (MilliporeSigma), washed with pre-cooled PBS and then fixed using 70% ethanol at 4˚C overnight. After washing with PBS, cells were incubated with 5 μl RNase A (10 mg/ml; Sigma-Aldrich; Merck KGaA) and 2.5 μl propidium iodide (5 mg/ml; Beyotime Institute of Biotechnology) for 30 min at room temperature in the dark. Finally, the cell cycle progression was analyzed using a BD FACSCalibur flow cytometer (BD Biosciences) before the percentage of cells at each phase of the cell cycle (G_0/G_1, S and G_2/M) was assessed using the FlowJo v.10.7.1 software (FlowJo LLC).

Western blotting. HeLa cells were lysed using RIPA buffer (Thermo Fisher Scientific, Inc.) to extract the total protein. Following determination of the protein concentration using a BCA assay (Beyotime Institute of Biotechnology), the proteins (25 μg per lane) were separated using 12% SDS-PAGE and then transferred onto PVDF membranes. After blocking using 5% skimmed milk for 1 h at room temperature, the membranes were probed overnight at 4˚C with primary antibodies against HBXIP (1:1,000; cat. no. ab157480; Abcam), FHL2 (1:1,000; cat. no. ab202584; Abcam), CyclinD1 (1:200; cat. no. ab16663; Abcam), CyclinD2 (1:1,000; cat. no. ab207604; Abcam), MMP2 (1:1,000; cat. no. ab92536; Abcam), MMP9 (1:1,000; cat. no. ab76003; Abcam), β-catenin (1:5,000; cat. no. ab32572; Abcam), c-Myc (1:1,000; cat. no. ab32072; Abcam), GAPDH (1:2,500; cat. no. ab9485; Abcam) and β-actin (1:1,000; cat. no. ab8227; Abcam). Membranes were then probed using the HRP-conjugated goat anti-rabbit IgG (1:2,000; cat. no. ab6721; Abcam) secondary antibodies for 2 h at room temperature. Pierce™ ECL Plus Western Blotting Substrate (Pierce; Thermo Fisher Scientific, Inc.) were used to visualize blots, followed by semi-quantification using ImageJ (version 1.46; National Institutes of Health) with GAPDH as the internal control.

Reverse transcription-quantitative PCR (RT-qPCR). The mRNA expression levels of HBXIP and FHL2 in HeLa cells were assessed using RT-qPCR. In brief, an RNeasy Universal Mini Kit (Qiagen GmbH) was used for the extraction of total RNA according to the manufacturer's protocol, followed by cDNA synthesis using a PrimeScript™ 1st strand cDNA Synthesis kit (Takara Bio, Inc.). The reverse transcription was performed at 37˚C for 30 min, followed by 85˚C for 5 sec and 4˚C for maintenance. Subsequently, qPCR was performed using SYBR Green PCR Master mix (Takara Bio, Inc.) in an ABI 7500 PCR system (Applied Biosystems; Thermo Fisher Scientific, Inc.). The thermocycling condition used were as follows: 95˚C for 10 min, followed by 40 cycles of 95˚C for 15 sec and 60˚C for 45 sec, then 95˚C for 15 sec, 60˚C for 1 min, 95˚C for 15 sec and 60˚C for 15 sec. The primer sequences used were as follows: HBXIP forward, 5'-GAGCCCAAGCCTTCGTCAG-3' and reverse, 5'-GGCACGTCCTTCTCCACCA-3'; FHL2 forward, 5'-GTACAGACTGCTATTCCAACGAG-3' and reverse, 5'-GCACTGCATGGCATGTTGTT-3' and GAPDH forward, 5'-CCATGGGGAAGGTGAAGGTC-3' and reverse, 5'-AGTGATGGCATGGACTGTGG-3'. The $2^{-\Delta\Delta Cq}$ method was used to assess the relative expression of aforementioned genes with GADPH as the constitutive internal control (23).

Co-immunoprecipitation (Co-IP) assay. HeLa cells were lysed on ice in RIPA lysis buffer (Thermo Fisher Scientific, Inc.) containing 1 μM PMSF protease inhibitor (Thermo Fisher Scientific, Inc.) for 30 min, followed by centrifugation at 13,000 x g for 15 min at 4˚C and supernatant collection. The lysates (500 μg) were incubated with a total of 1 μg antibodies targeting HBXIP (1:100; cat. no. sc-373980; Santa Cruz Biotechnology, Inc.) and FHL2 (1:30; cat. no. ab202584; Abcam) and then rotated at 4˚C with a mixture of 30 μl protein A/G agarose beads for an additional incubation at 4˚C overnight. After the IP reaction, 30 μl agarose beads were centrifuged at 1,000 x g for 3 min at 4˚C to the bottom of the tube. The supernatant was then carefully absorbed, and the agarose beads were washed three times with 1 ml lysis buffer. A total of 15 μl 2X SDS sample buffer was finally added for boiling at 100˚C for 5 min, followed by analysis by western blotting according to the aforementioned protocol.

Statistical analysis. All experimental data are represented by at least three independent experimental repeats and are presented as the mean ± standard deviation and were assessed using GraphPad Prism 8.0 (GraphPad Software, Inc.). One-way ANOVA followed by Tukey's post hoc test was used to assess the differences among multiple groups. $P<0.05$ was considered to indicate a statistically significant difference.

Results

HBXIP is highly expressed in cervical cancer cells. RT-qPCR and western blotting demonstrated a marked elevation in the HBXIP mRNA and protein expression levels in HeLa, C33A, Ca-Ski and SiHa cervical cancer cell lines compared with those in the End1/E6E7 human cervical epithelial cell line (Fig. 1). In particular, the HeLa cell line exhibited the highest mRNA and protein expression levels of HBXIP (Fig. 1). Therefore, it was chosen for subsequent experiments.

HBXIP knockdown inhibits the proliferation of cervical cancer cells. HBXIP expression in HeLa cells was subsequently knocked down and it was demonstrated that the HBXIP mRNA and protein expression levels were significantly reduced compared with those in the siRNA-NC group (Fig. 2A and B). Since siRNA-HBXIP-1 resulted in higher knockdown efficiency, siRNA-HBXIP-1 was chosen for subsequent experiments, which was referred to as 'siRNA-HBXIP' thereafter. Compared with that in the siRNA-NC group, a significant decrease in cell viability was observed in the siRNA-HBXIP group at both 48 and 72 h (Fig. 2C). Furthermore, EDU staining revealed markedly decreased levels of cell proliferation in the siRNA-HBXIP group compared with that in the siRNA-NC group (Fig. 2D).

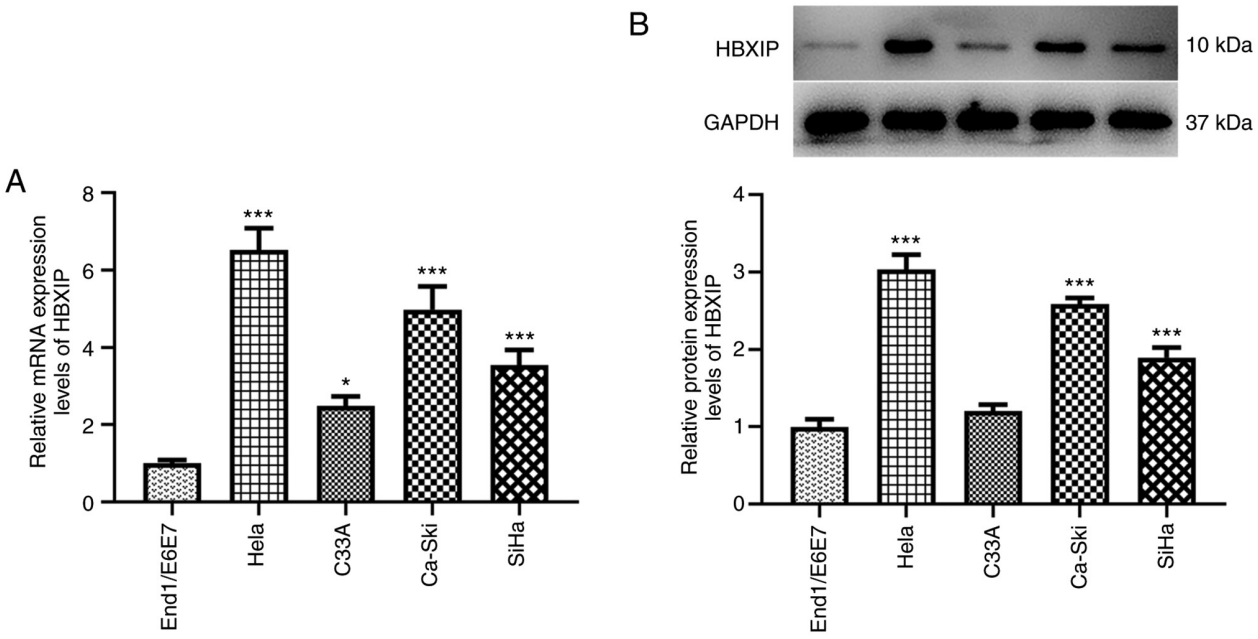

Figure 1. HBXIP is highly expressed in cervical cancer cells. HBXIP (A) mRNA and (B) protein expression levels were assessed in cervical cancer cell lines using reverse transcription-quantitative PCR and western blotting, respectively. *P<0.05 and ***P<0.001 vs. End1/E6E7. HBXIP, hepatitis B X-interacting protein.

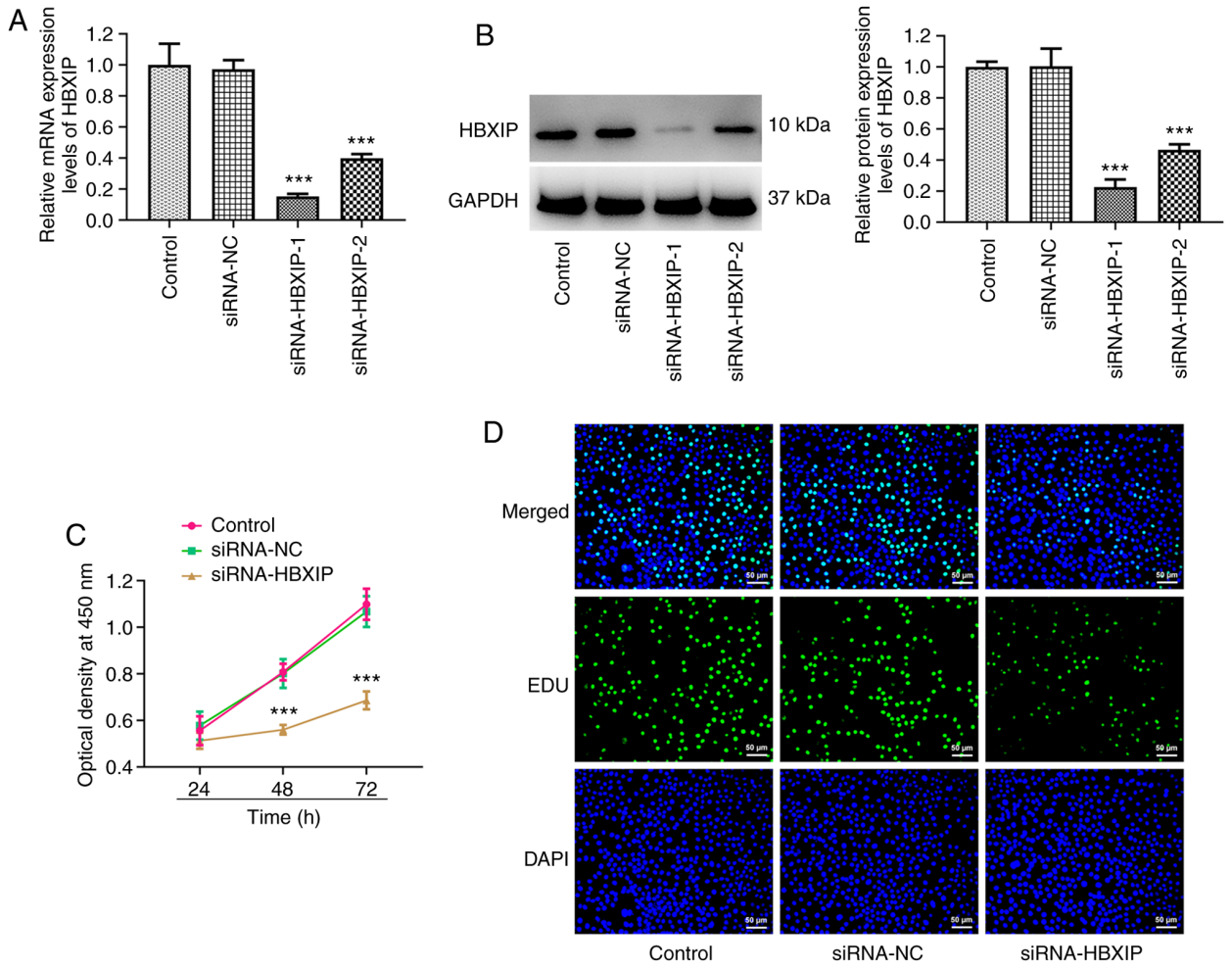

Figure 2. HBXIP knockdown inhibits the proliferation of cervical cancer cells. The knockdown efficiency of HBXIP was assessed using (A) reverse transcription-quantitative PCR and (B) western blotting. (C) Cell viability of HeLa cells was assessed using a Cell Counting Kit-8 assay after HBXIP knockdown. (D) Cell proliferation was assessed using EDU staining and a fluorescence microscope. Scale bars, 50 μm. ***P<0.001 vs. siRNA-NC. EDU, 5-ethynyl-2'-deoxyuridine; HBXIP, hepatitis B X-interacting protein; NC, negative control; siRNA, small interfering RNA.

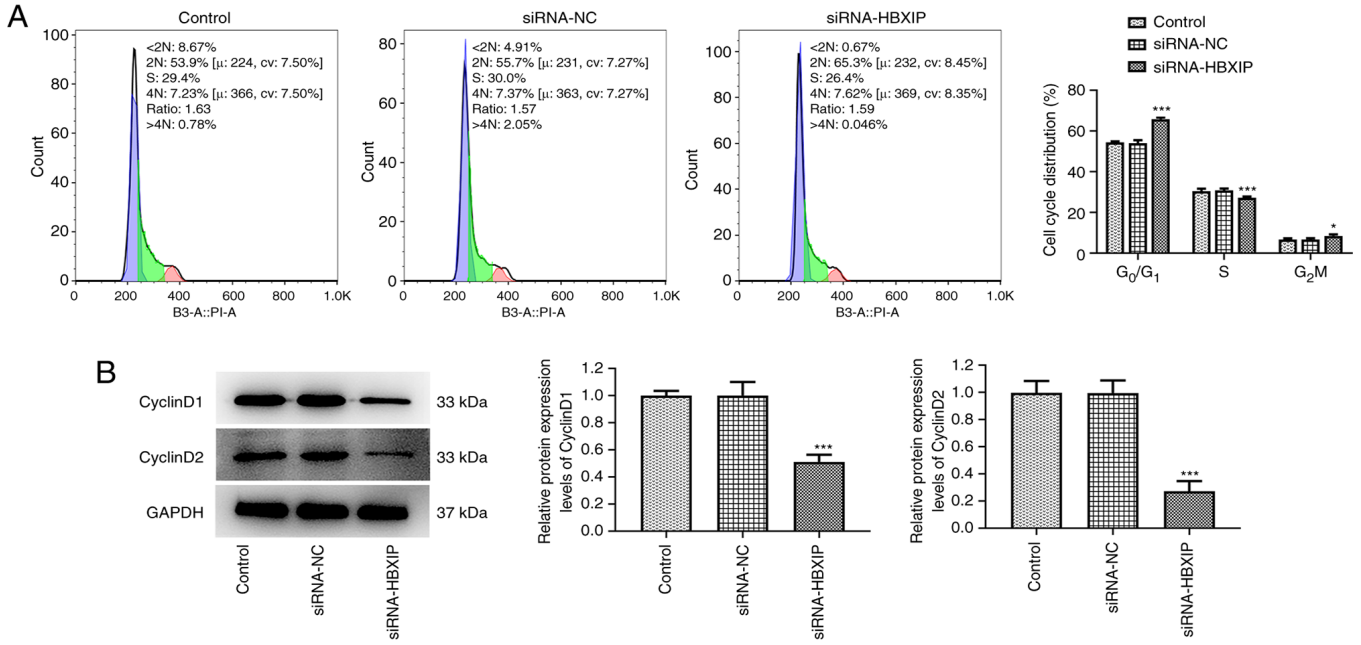

Figure 3. HBXIP knockdown promotes G_0/G_1 cycle arrest in cervical cancer cells. (A) HeLa cell cycle progression was assessed using flow cytometry after HBXIP knockdown. (B) Protein expression levels of CyclinD1 and CyclinD2 were assessed using western blotting. *P<0.05 and ***P<0.001 vs. siRNA-NC. HBXIP, hepatitis B X-interacting protein; NC, negative control; siRNA, small interfering RNA; PI, propidium iodide; cv, coefficient of variation.

HBXIP knockdown promotes G_0/G_1 cycle arrest in cervical cancer cells. HBXIP knockdown significantly promoted the cell cycle arrest of HeLa cells at the G_0/G_1 phase, slightly accelerated cell cycle arrest at the G_2/M phase and slightly obstructed cell cycle arrest at the S phase compared with that in the siRNA-NC group (Fig. 3A). Furthermore, the protein expression levels of CyclinD1 and CyclinD2, which are associated with G_1/S phase cell-cycle transition (24), were significantly reduced in HeLa cells transfected with siRNA-HBXIP compared with those in the siRNA-NC group (Fig. 3B).

HBXIP knockdown suppresses the invasion and migration of cervical cancer cells. The migration rate was significantly decreased in HeLa cells following the knockdown of HBXIP expression compared with that in the siRNA-NC group (Fig. 4A). Similarly, the number of invasive cells was also significantly decreased in the siRNA-HBXIP group compared with that in the siRNA-NC group (Fig. 4B). Furthermore, the protein expression levels of cell invasion markers MMP2 and MMP9 were significantly decreased in HBXIP-knockdown HeLa cells compared with those in the siRNA-NC group (Fig. 4C).

FHL2 overexpression reverses the inhibitory effects of HBXIP knockdown on the proliferation of cervical cancer cells. The BioGRID database predicted that FHL2 was likely to bind to HBXIP. Similarly to HBXIP, FHL2 also demonstrated high mRNA and protein expression levels in cervical cancer cell lines, especially in HeLa cells, where its mRNA and protein expression levels were significantly increased compared with those in End1/E6E7 cells apart from C33A cells (Fig. 5A and B). FHL2 mRNA and protein expression levels in HeLa cells were significantly downregulated after HBXIP knockdown compared with those in the siRNA-NC group (Fig. 5C and D). Furthermore, Co-IP demonstrated the interaction between HBXIP and FHL2 (Fig. 5E). Significant elevations in FHL2 mRNA and protein expression was demonstrated after Ov-FHL2 was transfected into HeLa cells compared with those in the Ov-NC group (Fig. 5F and G). Subsequently, HeLa cells co-transfected with siRNA-HBXIP and Ov-FHL2 demonstrated significantly enhanced cell viability at 72 h compared with that in the siRNA-HBXIP + Ov-NC group (Fig. 5H). The EDU staining results were also consistent with the trend of changes observed in the cell viability assay (Fig. 5I).

FHL2 overexpression reverses the promoting effects of HBXIP knockdown on cervical cancer cell cycle arrest. The results of the flow cytometry assay demonstrated that overexpression of FHL2 significantly decreased the number of cells at the G_0/G_1 phase and G_2/M phase, and increased the number of cells at the S phase compared with that in the siRNA-HBXIP + Ov-NC group (Fig. 6A and B). Furthermore, western blotting revealed significantly increased CyclinD1 and CyclinD2 protein expression levels in HeLa cells co-transfected with siRNA-HBXIP and Ov-FHL2 compared with those in the siRNA-HBXIP + Ov-NC group (Fig. 6C).

FHL2 overexpression counteracts the inhibitory effects of HBXIP knockdown on cervical cancer cell invasion and migration. The migration and invasion of HeLa cells were demonstrated to be significantly enhanced in the siRNA-HBXIP + Ov-FHL2 group compared with that in the siRNA-HBXIP + Ov-NC group (Fig. 7A and B). Furthermore, compared with those in the siRNA-HBXIP + Ov-NC group, it was demonstrated that the protein expression levels of MMP2 and MMP9 were significantly elevated following FHL2 overexpression in HBXIP-knockdown HeLa cells (Fig. 7C).

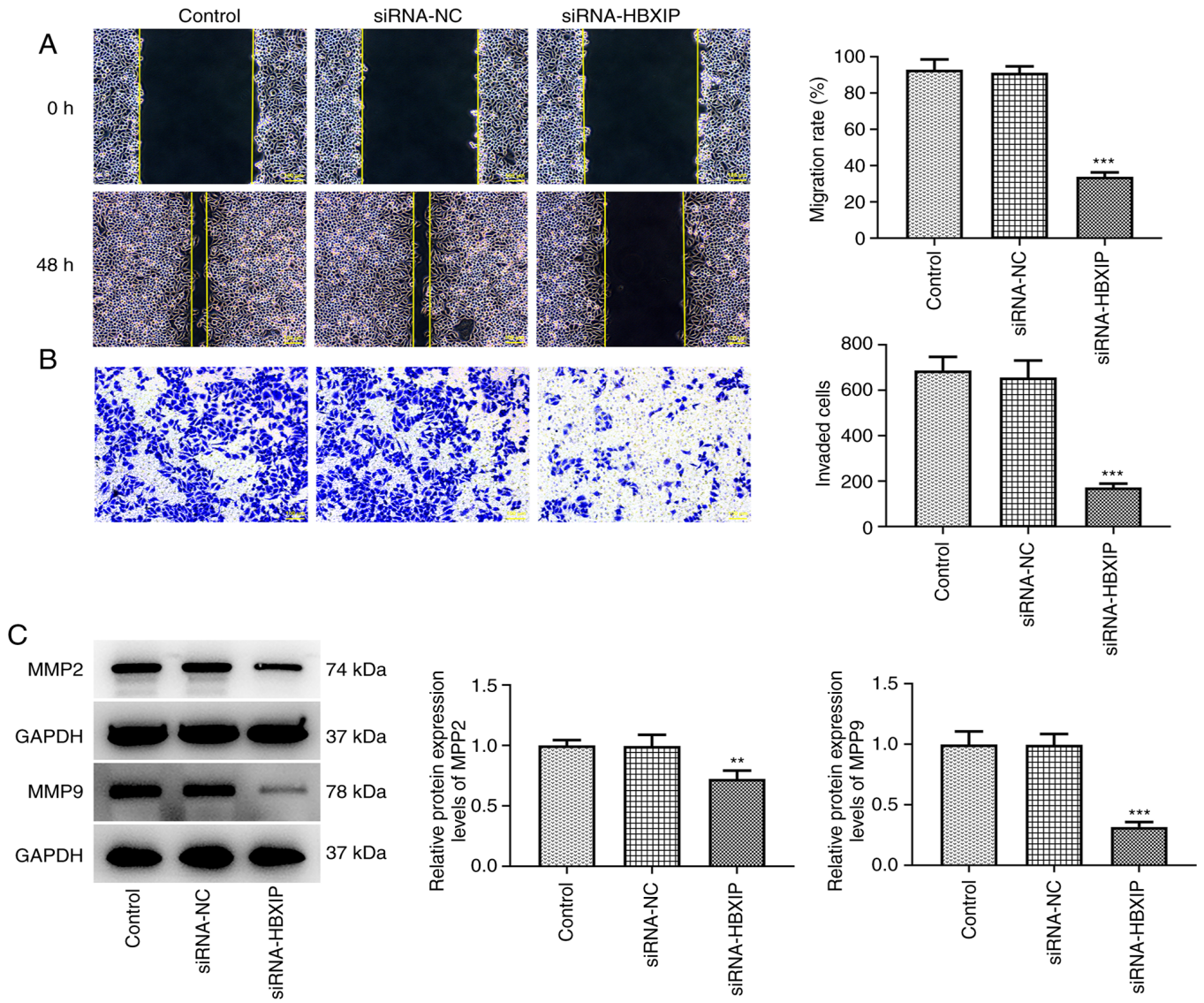

Figure 4. HBXIP knockdown suppresses the invasion and migration of cervical cancer cells. (A) Migration and (B) invasion of HBXIP-knockdown HeLa cells were assessed using wound healing and Transwell assays, respectively. The images were captured under a light microscope. Scale bars, 100 μm. (C) Protein expression levels of MMP2 and MMP9 were assessed using western blotting. **P<0.01 and ***P<0.001 vs. siRNA-NC. HBXIP, hepatitis B X-interacting protein; NC, negative control; siRNA, small interfering RNA.

HBXIP knockdown inhibits Wnt signaling and is counteracted by FHL2 overexpression. To evaluate the potential regulatory mechanism, markers of the Wnt/β-catenin signaling pathway in HeLa cells was assessed after HBXIP knockdown and/or FHL2 overexpression. The protein expression levels of the Wnt/β-catenin signaling marker proteins β-catenin and c-Myc were demonstrated to be significantly reduced in HeLa cells transfected with siRNA-HBXIP compared with those in the siRNA-NC group (Fig. 8A). By contrast, this downregulated protein expression levels of β-catenin and c-Myc caused by siRNA-HBXIP transfection were significantly reversed by co-transfection with Ov-FHL2 compared with those in the siRNA-HBXIP + Ov-NC group (Fig. 8B).

Discussion

Cervical cancer has high mortality rates among women in low and middle-income countries (1). Although a previous study has reported the oncogenic mechanisms of HBXIP in a variety of tumors (10), the effects of HBXIP on tumor progression in cervical cancer have not been previously elucidated. Therefore, the present study attempted to elucidate the pathogenic mechanism of HBXIP in cervical cancer to further the understanding of tumor progression in cervical cancer.

The present study demonstrated that HBXIP mRNA level was significantly upregulated in cervical cancer cells (Hela, C33A and SiHa cells) and the cervical squamous cell carcinoma Ca-Ski cell line, while its protein level was significantly upregulated in Hela, Ca-Ski and SiHa cells, which is consistent with the results of a previous study (11) in which immunohistochemical and immunofluorescence staining showed that HBXIP expression was higher in cervical intraepithelial neoplasia and cervical cancer cells. During the development of cancer, cells can invade and spread to surrounding tissues and blood vessels through proliferation and migration (25,26). The prognosis of patients with cervical cancer is associated with

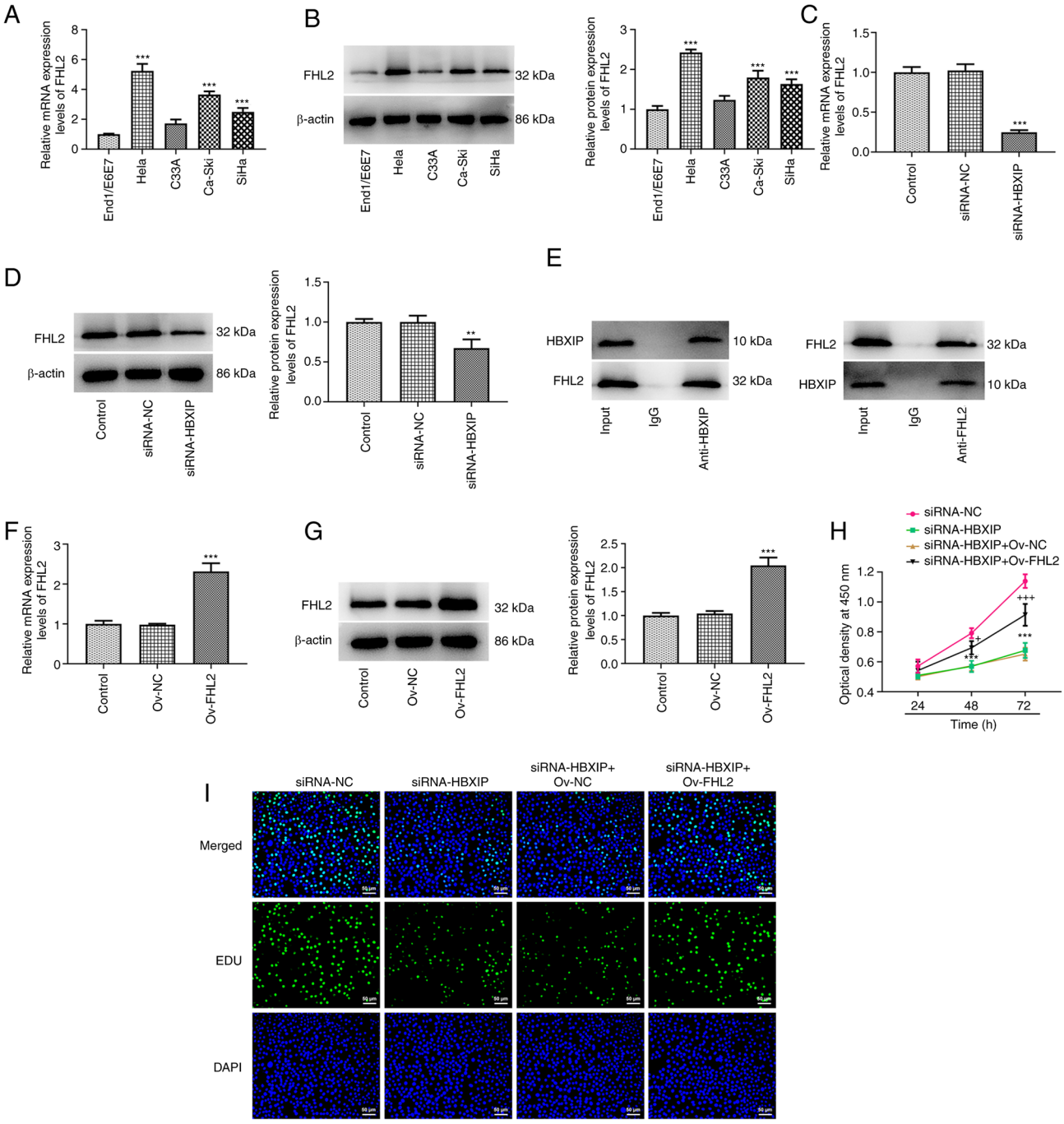

Figure 5. FHL2 overexpression reverses the inhibitory effects of HBXIP on the proliferation of cervical cancer cells. FHL2 (A) mRNA and (B) protein expression levels were assessed in cervical cancer cell lines using RT-qPCR and western blotting. ***P<0.001 vs. End1/E6E7. FHL2 (C) mRNA and (D) protein expression levels were assessed after HBXIP knockdown using RT-qPCR and western blotting, respectively. **P<0.01 and ***P<0.001 vs. siRNA-NC. (E) Relationship between HBXIP and FHL2 was evaluated using co-immunoprecipitation assay. The overexpression efficiency of FHL2 was assessed in HeLa cells using (F) RT-qPCR and (G) western blotting. ***P<0.001 vs. Ov-NC. (H) Cell viability of HeLa cells co-transfected with siRNA-HBXIP and Ov-FHL2 was assessed using a Cell Counting Kit-8 assay. ***P<0.001 vs. siRNA-NC; +P<0.05 and +++P<0.001 vs. siRNA-HBXIP + Ov-NC. (I) Cell proliferation levels were assessed in HeLa cells using EDU staining and were observed using a fluorescence microscope. Scale bars, 50 μm. EDU, 5-ethynyl-2'-deoxyuridine; FHL2, four and a half LIM domain 2; HBXIP, hepatitis B X-interacting protein; NC, negative control; Ov, overexpression; RT-qPCR, reverse transcription-quantitative PCR; siRNA, small interfering RNA.

the degree of tumor cell proliferation, local infiltration and metastasis (27). Numerous studies have previously reported that HBXIP upregulation can promote the tumor cell proliferation, migration and invasion capabilities by triggering various signaling pathways, such as the PI3K/AKT, ERK1/2 and NF-κB (28-30). However, knockdown of HBXIP may inhibit the malignant behaviors of tumor cells. HBXIP silencing has been reported to be associated with decreased methyltransferase 3 and N6-adenosine-methyltransferase complex catalytic subunit expression, which resulted in the repression of the proliferation, migration and invasion of gastric cancer cells (5). To evaluate this hypothesis, HBXIP expression was knocked down in HeLa cells in the present study, which resulted in cell proliferation, invasion and migration being

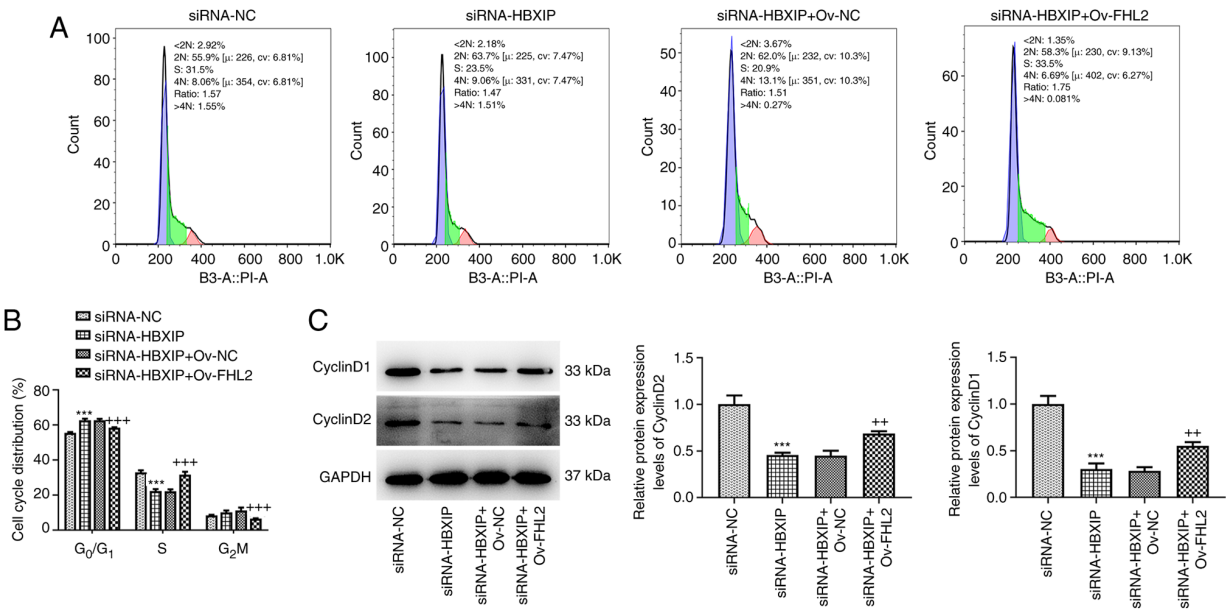

Figure 6. FHL2 overexpression reverses the promoting effects of HBXIP on cervical cancer cell cycle arrest. (A) Cell cycle distribution was assessed in Hela cells using flow cytometry after HBXIP knockdown and FHL2 overexpression, (B) which were then quantified. (C) Protein expression levels of CyclinD1 and CyclinD2 were assessed in HeLa cells after HBXIP knockdown and FHL2 overexpression using western blotting. ***P<0.001 vs. siRNA-NC; $^{++}$P<0.01 and $^{+++}$P<0.001 vs. siRNA-HBXIP + Ov-NC. FHL2, four and a half LIM domain 2; HBXIP, hepatitis B X-interacting protein; NC, negative control; Ov, overexpression; siRNA, small interfering RNA; PI, propidium iodide; cv, coefficient of variation.

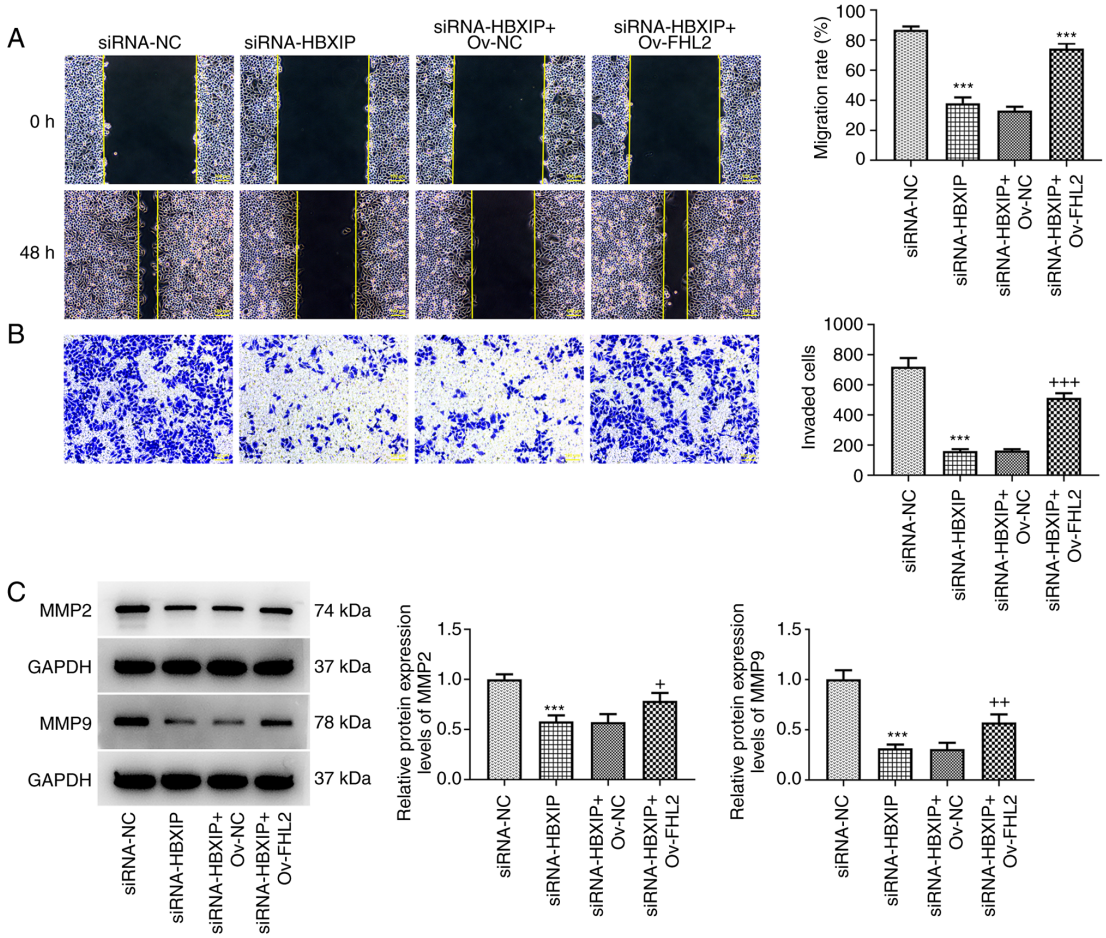

Figure 7. FHL2 overexpression reverses the inhibitory effects of HBXIP on cervical cancer cell invasion and migration. (A) Migration and (B) invasion of HeLa cells co-transfected with siRNA-HBXIP and Ov-FHL2 were assessed using wound healing and Transwell assays, respectively. The images were captured using a light microscope. Scale bars, 100 μm. (C) Protein expression levels of MMP2 and MMP9 were assessed in HeLa cells co-transfected with siRNA-HBXIP and Ov-FHL2 using western blotting. ***P<0.001 vs. siRNA-NC; $^{+}$P<0.05, $^{++}$P<0.01 and $^{+++}$P<0.001 vs. siRNA-HBXIP + Ov-NC. FHL2, four and a half LIM domain 2; HBXIP, hepatitis B X-interacting protein; NC, negative control; Ov, overexpression; siRNA, small interfering RNA.

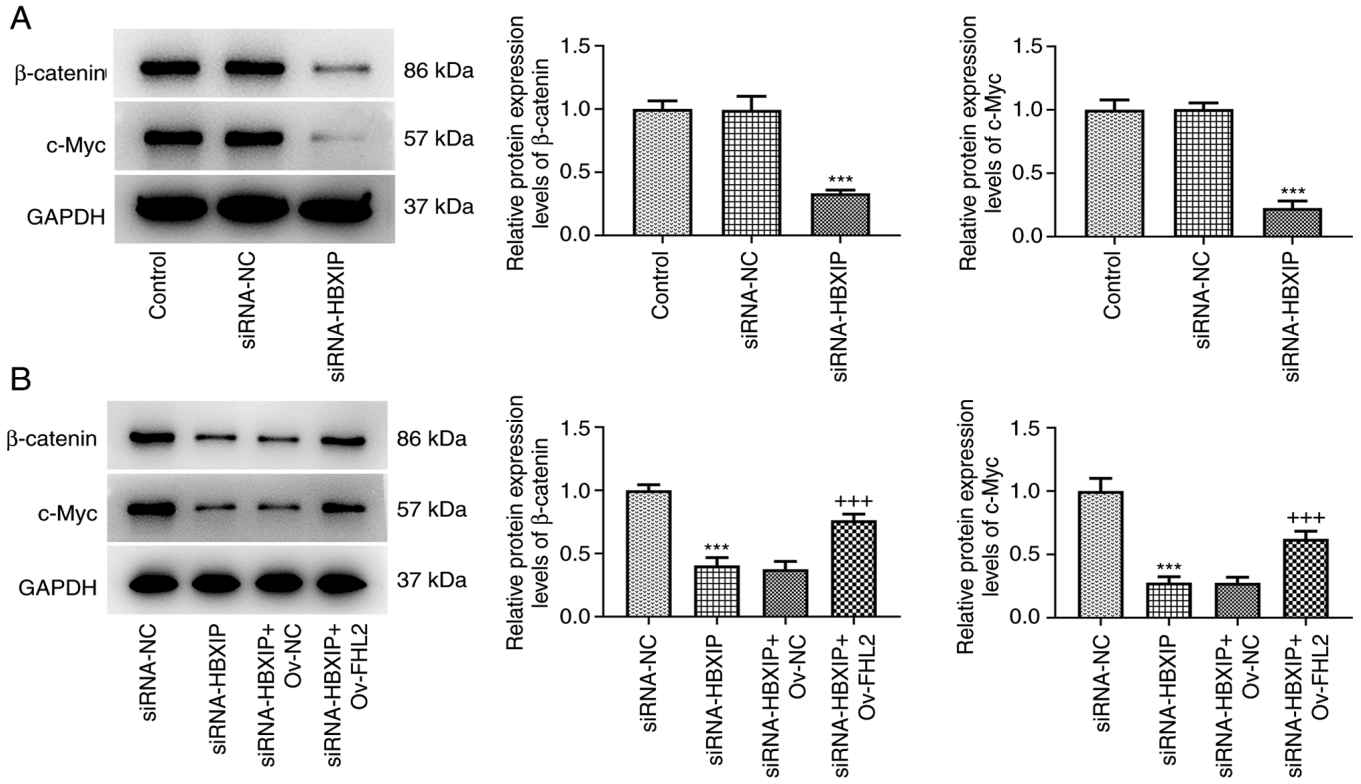

Figure 8. HBXIP knockdown inhibits Wnt signaling and is counteracted by FHL2 overexpression. The protein expression levels of β-catenin and c-Myc were assessed in (A) HBXIP-knockdown HeLa cells and (B) in HeLa cells co-transfected with siRNA-HBXIP and Ov-FHL2 using western blotting. ***P<0.001 vs. siRNA-NC; +++P<0.001 vs. siRNA-HBXIP + Ov-NC. FHL2, four and a half LIM domain 2; HBXIP, hepatitis B X-interacting protein; NC, negative control; Ov, overexpression; siRNA, small interfering RNA.

significantly decreased. This was also accompanied by the significantly decreased protein expression levels of cell migration markers MMP2 and MMP9. These results suggest that HBXIP served an important role in the physiology of cervical cancer.

Abnormalities in cell cycle progression can lead to uncontrolled cell proliferation and conversion to tumor cells (31). It has been reported that HBXIP can act as a mediator of DNA damage response signals and activate the G_2/M checkpoint to maintain genomic integrity (32). HBXIP has also been reported to indirectly upregulate cyclin D1 expression to promote hepatocellular carcinoma tumor growth through the PI3K/Akt pathway (28). However, HBXIP knockdown has been reported to abrogate ionizing radiation-induced G_2/M cell cycle checkpoints, sensitize osteosarcoma and liver cancer cells to chemotherapy and regulate cell cycle progression through modulating the DNA damage response (32). In the present study, HBXIP knockdown significantly promoted cell cycle arrest in cervical cancer cells at the G_0/G_1 and G_2/M phases with reduced the cell proportion in S phase. A corresponding decrease in cyclin D1 and cyclin D2 protein expression was also found. These results indicate that HBXIP served a role in the facilitation of cell cycle arrest in cervical cancer.

In the present study, evaluation using the BioGRID database predicted that FHL2 was likely to bind to HBXIP, which was then demonstrated using Co-IP in the present study. FHL2 has been reported to be highly expressed in cervical cancer cells (19,20), which was supported by the results of the present study. The effects of FHL2 on tumor progression have been reported to be regulated by a number of transcription factors, such as P53, serum response factor, specificity protein 1 and activator protein-1. They have been found to be involved in various biological functions, including cell adhesion, apoptosis, invasion, proliferation and differentiation (21). In addition, FHL2 overexpression can promote cell proliferation, migration and invasion in cancer types such as epithelial ovarian cancer, ovarian granulosa cell tumor and hepatocellular carcinoma (33-35). In the present study, FHL2 overexpression significantly abrogated the inhibitory effects of HBXIP knockdown on the proliferation, migration and invasion of HeLa cells, suggesting that HBXIP knockdown exerted suppressive effects on the malignant behavior of HeLa cells at least partially through the downregulation of FHL2 expression.

Wnt/β-catenin signaling has been reported to regulate several important cellular functions, including cell proliferation, differentiation, invasion, migration and metastasis (36). Wnt can bind the stabilizing transcription factor β-catenin, which can enter the nucleus to regulate the expression of target genes, such as Axin2, c-Myc and cyclin D1, which are associated with tumorigenesis (37). FHL2 has been reported to regulate the Wnt/β-catenin signaling pathway by increasing β-catenin dephosphorylation at the Ser37/Thr41 site and nuclear translocation to upregulate the β-catenin-mediated transcription of its target genes in rat tubular epithelial cells (38). Furthermore, HBXIP has been previously reported to induce the dysregulation of c-Myc, c-Jun and p53 mRNA and protein levels to promote tumor progression, such as

that of breast cancer, hepatocellular carcinoma and gastric cancer (10). In the present study, HBXIP knockdown was demonstrated to significantly inhibit FHL2 mRNA and protein expression. In addition, knockdown of HBXIP inhibited the expression of β-catenin and c-Myc, which was reversed by the overexpression of FHL2, suggesting that HBXIP knockdown suppressed Wnt/β-catenin signaling by downregulating FHL2.

The main limitation of the present study was the lack of *in vivo* verification. Future *in vivo* research would be beneficial to verify the results of the present study. Further studies are needed to further explore the precise oncogenic function and molecular mechanism of HBXIP-induced carcinogenesis.

Considering all the data, the present study has provided an evaluation of the role of HBXIP in cervical cancer. HBXIP knockdown repressed cervical cancer cell proliferation, invasion and migration, possibly by inhibiting Wnt/β-catenin signaling and downregulating FHL2 expression. The present study revealed that HBXIP or FHL2 might be function as a potential therapeutic target biomarker for cervical cancer therapy.

Acknowledgements

Not applicable.

Funding

No funding was received.

Availability of data and materials

The datasets used and/or analyzed during the current study are available from the corresponding author on reasonable request.

Authors' contributions

XG conceived and designed the study. XG performed the functional experiments and LY performed the mechanism assays. XG and LY collected the data. LY analyzed and interpreted the data, and drafted the manuscript. XG revised the manuscript. XG and LY confirm the authenticity of all the raw data. Both authors read and approved final manuscript.

Ethics approval and consent to participate

Not applicable.

Patient consent for publication

Not applicable.

Competing interests

The authors declare that they have no competing interests.

References

1. Lopez MS, Baker ES, Maza M, Fontes-Cintra G, Lopez A, Carvajal JM, Nozar F, Fiol V and Schmeler KM: Cervical cancer prevention and treatment in Latin America. J Surg Oncol 115: 615-618, 2017.
2. Canfell K, Kim JJ, Brisson M, Keane A, Simms KT, Caruana M, Burger EA, Martin D, Nguyen DTN, Bénard É, *et al*: Mortality impact of achieving WHO cervical cancer elimination targets: A comparative modelling analysis in 78 low-income and lower-middle-income countries. Lancet 395: 591-603, 2020.
3. Johnson CA, James D, Marzan A and Armaos M: Cervical cancer: An overview of pathophysiology and management. Semin Oncol Nurs 35: 166-174, 2019.
4. Zimet GD, Rosberger Z, Fisher WA, Perez S and Stupiansky NW: Beliefs, behaviors and HPV vaccine: Correcting the myths and the misinformation. Prev Med 57: 414-418, 2013.
5. Yang Z, Jiang X, Li D and Jiang X: HBXIP promotes gastric cancer via METTL3-mediated MYC mRNA m6A modification. Aging (Albany NY) 12: 24967-24982, 2020.
6. Zheng S, Wu H, Wang F, Lv J, Lu J, Fang Q, Wang F, Lu Y, Zhang S, Xu Y, *et al*: The oncoprotein HBXIP facilitates metastasis of hepatocellular carcinoma cells by activation of MMP15 expression. Cancer Manag Res 11: 4529-4540, 2019.
7. Zhao Y, Li H, Zhang Y, Li L, Fang R, Li Y, Liu Q, Zhang W, Qiu L, Liu F, *et al*: Oncoprotein HBXIP modulates abnormal lipid metabolism and growth of breast cancer cells by activating the LXRs/SREBP-1c/FAS signaling cascade. Cancer Res 76: 4696-4707, 2016.
8. Qiu L, Lu F, Zhang L, Wang G, Geng R and Miao Y: HBXIP regulates gastric cancer glucose metabolism and malignancy through PI3K/AKT and p53 signaling. Onco Targets Ther 13: 3359-3374, 2020.
9. Wang X, Feng Q, Yu H, Zhou X, Shan C, Zhang Q and Liu S: HBXIP: A potential prognosis biomarker of colorectal cancer which promotes invasion and migration via epithelial-mesenchymal transition. Life Sci 245: 117354, 2020.
10. Xiu M, Zeng X, Shan R, Wen W, Li J and Wan R: The oncogenic role of HBXIP. Biomed Pharmacother 133: 111045, 2021.
11. Li N, Wang Y, Che S, Yang Y, Piao J, Liu S and Lin Z: HBXIP over expression as an independent biomarker for cervical cancer. Exp Mol Pathol 102: 133-137, 2017.
12. Chan KK, Tsui SK, Lee SM, Luk SC, Liew CC, Fung KP, Waye MM and Lee CY: Molecular cloning and characterization of FHL2, a novel LIM domain protein preferentially expressed in human heart. Gene 210: 345-350, 1998.
13. Kinoshita M, Nakagawa T, Shimizu A and Katsuoka Y: Differently regulated androgen receptor transcriptional complex in prostate cancer compared with normal prostate. Int J Urol 12: 390-397, 2005.
14. Genini M, Schwalbe P, Scholl FA, Remppis A, Mattei MG and Schäfer BW: Subtractive cloning and characterization of DRAL, a novel LIM-domain protein down-regulated in rhabdomyosarcoma. DNA Cell Biol 16: 433-442, 1997.
15. Xu J, Zhou J, Li MS, Ng CF, Ng YK, Lai PBS and Tsui SKW: Transcriptional regulation of the tumor suppressor FHL2 by p53 in human kidney and liver cells. PLoS One 9: e99359, 2014.
16. Gabriel B, Mildenberger S, Weisser CW, Metzger E, Gitsch G, Schüle R and Müller JM: Focal adhesion kinase interacts with the transcriptional coactivator FHL2 and both are overexpressed in epithelial ovarian cancer. Anticancer Res 24: 921-927, 2004.
17. Chan KK, Tsui SK, Ngai SM, Lee SM, Kotaka M, Waye MM, Lee CY and Fung KP: Protein-protein interaction of FHL2, a LIM domain protein preferentially expressed in human heart, with hCDC47. J Cell Biochem 76: 499-508, 2000.
18. Chen D, Xu W, Bales E, Colmenares C, Conacci-Sorrell M, Ishii S, Stavnezer E, Campisi J, Fisher DE, Ben-Ze'ev A and Medrano EE: SKI activates Wnt/beta-catenin signaling in human melanoma. Cancer Res 63: 6626-6634, 2003.
19. Jin H, Lee K, Kim YH, Oh HK, Maeng YI, Kim TM, Suh DS and Bae J: Scaffold protein FHL2 facilitates MDM2-mediated degradation of IER3 to regulate proliferation of cervical cancer cells. Oncogene 35: 5106-5118, 2016.
20. Jin X, Jiao X, Jiao J, Zhang T and Cui B: Increased expression of FHL2 promotes tumorigenesis in cervical cancer and is correlated with poor prognosis. Gene 669: 99-106, 2018.
21. Cao CY, Mok SWF, Cheng VWS and Tsui SKW: The FHL2 regulation in the transcriptional circuitry of human cancers. Gene 572: 1-7, 2015.
22. Brun J, Dieudonné FX, Marty C, Müller J, Schüle R, Patiño-García A, Lecanda F, Fromigué O and Marie PJ: FHL2 silencing reduces Wnt signaling and osteosarcoma tumorigenesis in vitro and in vivo. PLoS One 8: e55034, 2013.
23. Livak KJ and Schmittgen TD: Analysis of relative gene expression data using real-time quantitative PCR and the 2(-Delta Delta C(T)) method. Methods 25: 402-408, 2001.

24. Qie S and Diehl JA: Cyclin D1, cancer progression, and opportunities in cancer treatment. J Mol Med (Berl) 94: 1313-1326, 2016.
25. Hamidi H and Ivaska J: Every step of the way: Integrins in cancer progression and metastasis. Nat Rev Cancer 18: 533-548, 2018.
26. Oudin MJ and Weaver VM: Physical and chemical gradients in the tumor microenvironment regulate tumor cell invasion, migration, and metastasis. Cold Spring Harb Symp Quant Biol 81: 189-205, 2016.
27. Nie H, Bu F, Xu J, Li T and Huang J: 29 immune-related genes pairs signature predict the prognosis of cervical cancer patients. Sci Rep 10: 14152, 2020.
28. Wang FZ, Fei HR, Lian LH, Wang JM and Qiu YY: Hepatitis B x-interacting protein induces HepG2 cell proliferation through activation of the phosphatidylinositol 3-kinase/Akt pathway. Exp Biol Med (Maywood) 236: 62-69, 2011.
29. Li Y, Zhang Z, Zhou X, Li L, Liu Q, Wang Z, Bai X, Zhao Y, Shi H, Zhang X and Ye L: The oncoprotein HBXIP enhances migration of breast cancer cells through increasing filopodia formation involving MEKK2/ERK1/2/Capn4 signaling. Cancer Lett 355: 288-296, 2014.
30. Wang Y, Cui M, Cai X, Sun B, Liu F, Zhang X and Ye L: The oncoprotein HBXIP up-regulates SCG3 through modulating E2F1 and miR-509-3p in hepatoma cells. Cancer Lett 352: 169-178, 2014.
31. Zheng K, He Z, Kitazato K and Wang Y: Selective autophagy regulates cell cycle in cancer therapy. Theranostics 9: 104-125, 2019.
32. Fei H, Zhou Y, Li R, Yang M, Ma J and Wang F: HBXIP, a binding protein of HBx, regulates maintenance of the G2/M phase checkpoint induced by DNA damage and enhances sensitivity to doxorubicin-induced cytotoxicity. Cell Cycle 16: 468-476, 2017.
33. Wang C, Lv X, He C, Davis JS, Wang C and Hua G: Four and a half LIM domains 2 (FHL2) contribute to the epithelial ovarian cancer carcinogenesis. Int J Mol Sci 21: 7751, 2020.
34. Hua G, He C, Lv X, Fan L, Wang C, Remmenga SW, Rodabaugh KJ, Yang L, Lele SM, Yang P, *et al*: The four and a half LIM domains 2 (FHL2) regulates ovarian granulosa cell tumor progression via controlling AKT1 transcription. Cell Death Dis 7: e2297, 2016.
35. Shao C, Qiu Y, Liu J, Feng H, Shen S, Saiyin H, Yu W, Wei Y, Yu L, Su W and Wu J: PARP12 (ARTD12) suppresses hepatocellular carcinoma metastasis through interacting with FHL2 and regulating its stability. Cell Death Dis 9: 856, 2018.
36. Duchartre Y, Kim YM and Kahn M: The Wnt signaling pathway in cancer. Crit Rev Oncol Hematol 99: 141-149, 2016.
37. Bahrami A, Amerizadeh F, ShahidSales S, Khazaei M, Ghayour-Mobarhan M, Sadeghnia HR, Maftouh M, Hassanian SM and Avan A: Therapeutic potential of targeting wnt/beta-catenin pathway in treatment of colorectal cancer: Rational and progress. J Cell Biochem 118: 1979-1983, 2017.
38. Cai T, Sun D, Duan Y, Qiu Y, Dai C, Yang J and He W: FHL2 promotes tubular epithelial-to-mesenchymal transition through modulating beta-catenin signalling. J Cell Mol Med 22: 1684-1695, 2018.